Available online at www.sciencedirect.com

ScienceDirect

Journal of Solid State Chemistry 181 (2008) 1025–1031

JOURNAL OF SOLID STATE CHEMISTRY

www.elsevier.com/locate/jssc

The excited state dynamics of $KLa(MoO_4)_2:Pr^{3+}$: From a case study to the determination of the energy levels of rare earth impurities relative to the bandgap in oxidising host lattices

Enrico Cavalli[a,*], Philippe Boutinaud[b], Marco Bettinelli[c], Pieter Dorenbos[d]

[a]Dipartimento di Chimica Generale ed Inorganica, Chimica Analitica, Chimica Fisica, Università di Parma, Parma, Italy
[b]Laboratoire des Matériaux Inorganiques—UMR 6002, Université Blaise-Pascal et ENSCCF, Aubière, France
[c]Dipartimento Scientifico e Tecnologico, Università di Verona and INSTM, UdR Verona, Verona, Italy
[d]Faculty of Applied Sciences, Delft University of Technology, Delft, The Netherlands

Received 23 November 2007; received in revised form 14 January 2008; accepted 14 February 2008
Available online 4 March 2008

Abstract

The luminescence properties of $KLa(MoO_4)_2$ (KLM) single crystals doped with Pr^{3+} have been measured in the 10–600 K temperature range in order to investigate the mechanisms involved in the radiationless processes. At variance with previously studied scheelite-like molybdates activated with Pr^{3+}, no effects attributed to the formation of intervalence charge transfer states have been observed. The model proposed in order to account for this behaviour allows the determination of the energy of the Pr^{3+} levels relative to the valence and conduction bands of the host. This model has firstly been confirmed for Tb^{3+}-doped KLM, for which suitable experimental data are available, and then extended to the other rare earth ions on the basis of the systematic nature of the lanthanide energy levels properties. The obtained conclusions are finally supported in the light of the comparison with some other representative cases.

Keywords: Luminescence; Praseodymium; Potassium lanthanum molybdate; Rare earths; Electronic structure

1. Introduction

$KLa(MoO_4)_2$ (hereafter KLM) is an interesting host material for luminescent rare earth ions, and it has been widely investigated in order to develop new solid state laser media [1–3]. It belongs to the scheelite family, and it is characterized by an intrinsic structural disorder resulting in a significant inhomogeneous broadening of the spectral features. Pr^{3+}-doped scheelite molybdate crystals were investigated in the late 1960s by Reut and Ryskin [4], who evidenced the effect of the formation of a Pr^{4+}–Mo^{5+} intervalence charge transfer (IVCT) state on the excited state dynamics. We have extended this study to other classes of crystals (vanadates, titanates, niobates, etc.) activated with Pr^{3+} and Tb^{3+}, and we have demonstrated the fundamental role played by the IVCT state in determining the de-excitation pathways in these materials [5,6]. We are then revisiting some compounds already investigated in the light of the new information available, in order to relate the formation of IVCT state to the properties of the host lattice. In this connection we have recently demonstrated that in Tb:KLM no IVCT processes take place, despite the favourable redox properties of Tb^{3+} and Mo^{6+} [7]. In this work we examine the case of Pr:KLM with the purpose of confirming previous results and of proposing a general model accounting for the observed behaviour and providing information about the position of the energy levels of the rare earth ion with respect to the bandgap of the host.

2. Experimental

Pr:KLM single crystals with 0.36% and 5% Pr/La nominal molar ratios were grown by the flux growth method [1]. The molar composition of the starting mixture

---

*Corresponding author. Fax: +39 0521 905436.
E-mail address: enrico.cavalli@unipr.it (E. Cavalli).

0022-4596/$ - see front matter © 2008 Elsevier Inc. All rights reserved.
doi:10.1016/j.jssc.2008.02.007

was 5.2% La_2O_3, 23.7% K_2CO_3, and 71.1% MoO_3. The dopant was added as Pr_6O_{11} in proper amount. The mixture was put in a platinum crucible and slowly heated to 1260 °C in a horizontal furnace. After a soaking time of 10 h, the temperature was lowered to 600 °C with a cooling rate of 3 °C/h, and then the furnace was turned off. After complete cooling, the crystals were separated from the flux by dissolving it in hot diluted NaOH. They have a tetragonal scheelite ($CaWO_4$) structure, with space group $I4_1/a$ and cell parameters $a = 5.445$ and $c = 12.208$ Å [2]. The K^+ and La^{3+} atoms are randomly distributed at the Ca^{2+} positions with eight-fold oxygen coordination (distorted dodecahedron, actual point symmetry S_4). Such a disorder affects the homogeneity of the crystal field around the optically active dopants, inducing a significant broadening of the absorption and emission features even in the low temperature spectra.

The emission spectra were measured in the 10−600 K temperature range using a Triax 550 monochromator equipped with a nitrogen-cooled CCD camera and a R928 Hamamatsu photomultiplier (Jobin-Yvon Symphony system). The excitation light was selected from a xenon lamp using a Triax 180 monochromator. The spectra in the 10−300 K range were obtained by cooling the samples by means of an He-closed cycle cryostat (Air Products Displex DE-202), those in the 300−600 K range with the help of a home-made copper holder heated by a thermocoax wire connected to a Thermolyne regulator. The decay profiles were measured in the 10–300 K temperature range upon 355 nm laser excitation using a pulsed Nd:YAG laser (Quanta System model SYL 202); the emission was isolated by means of a Hilger–Watts model D330 double monochromator and detected with a Hamamatsu R943-022 photomultiplier connected to a LeCroy 9410 transient digitizer. The Raman spectrum of KLM was measured with a Renishaw Raman spectrometer using the 514 nm radiation from an Ar^+ laser.

3. Experimental results

3.1. Spectral properties of the host

We have measured some spectral properties of previously grown pure KLM crystals, since they are useful in the analysis of the spectra of the compound under investigation. KLM exhibits at low temperature a broad-band emission with maximum at about 650 nm (Fig. 1) The excitation maximum is at 320 nm. At room temperature, KLM is nearly not luminescent. Its emission is assigned to a charge transfer process involving the transfer of one electron from an oxygen ligand to the coordinated Mo^{6+} ion [8]. The Stokes shift is relatively large, about 15 800 cm^{-1}. The Raman spectrum (Fig. 2) has been measured in order to identify the phonon energies that could be involved in non-radiative processes. This spectrum is composed of two band systems in the 350 and 950 cm^{-1} regions. The transitions have been assigned in terms of normal modes of the tetrahedral MoO_4^{2-} unit, in agreement with previous literature [9]. The highest phonon energies in this material are at about 910 and 940 cm^{-1}.

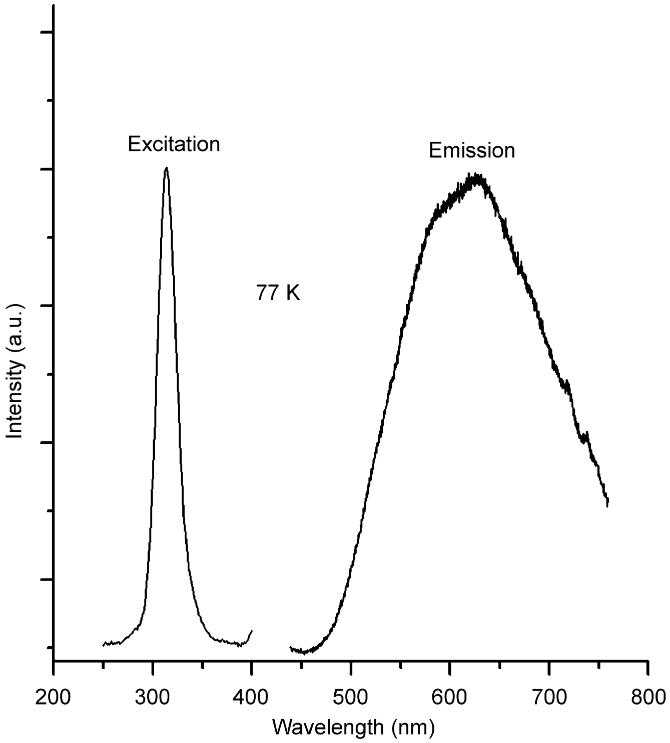

Fig. 1. Excitation and emission spectra of the MoO_4^{2-} ion in KLM. The spectra are not calibrated for the system responsivity.

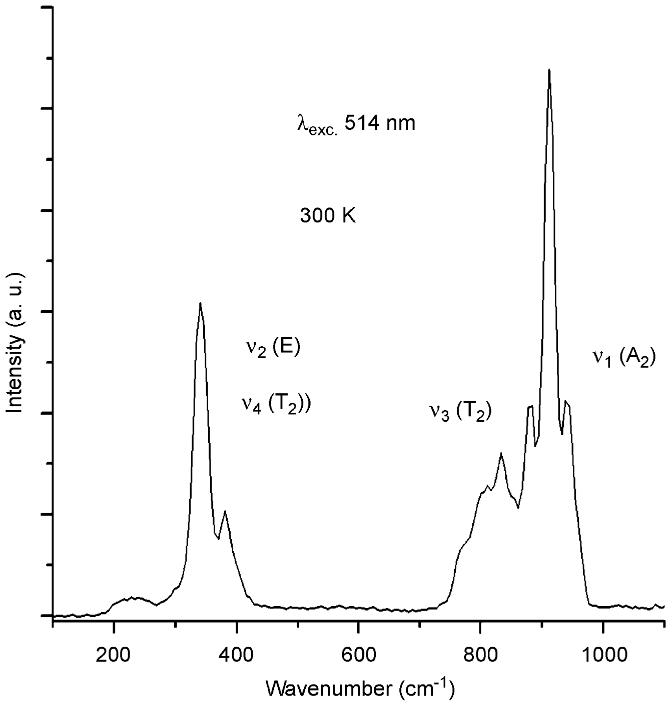

Fig. 2. Raman spectrum of KLM.

3.2. The 10 K emission spectra of Pr:KLM

The 10 K emission spectra of diluted (0.36%) and concentrated (5%) Pr:KLM are presented in Fig. 3. All observed features are significantly in homogeneously broadened as a consequence of the structural disorder. They have been assigned according to previous literature [10] and summarised in the inset of Fig. 3. It can be noted that the energy gap between the $^3P_0$ and $^1D_2$ emitting levels is compatible with a multiphonon emission process, since it can be bridged by about four high energy phonons present in the Raman spectrum. It can also be pointed out that the relatively high intensity of the $^3P_0 \rightarrow {}^3F_2$ hypersensitive transition is consistent with the high value of the second order intensity parameter calculated by Macalik et al. [10], as observed in the cases of the Tm- and Nd-doped KLM crystals [1,2]. The small differences in the $^3P_0$ emission features of the two crystals can be ascribed to clustering effects. The transition from the $^1D_2$ state is very weak in the spectrum of the 5% doped sample. The emission from this level is, in fact, affected by concentration quenching to a much greater extent than that from $^3P_0$. The main mechanisms accounting for the concentration quenching of both levels are the cross-relaxation processes:

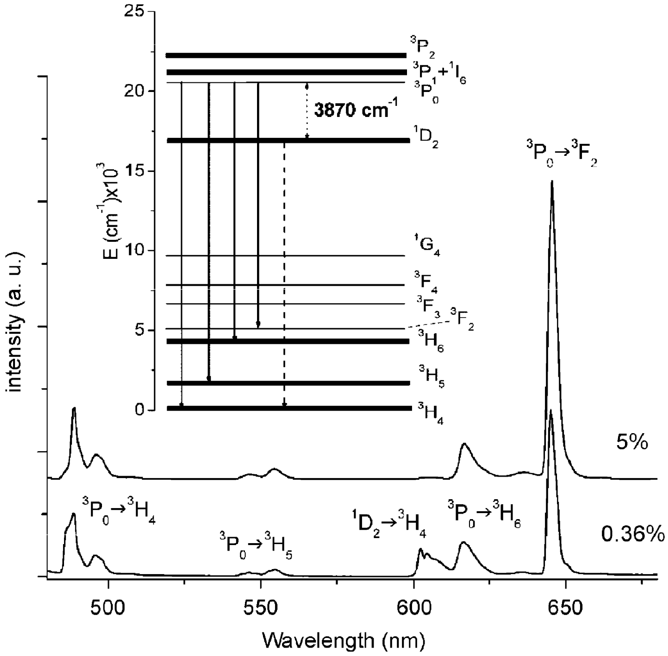

Fig. 3. The 10 K emission spectra of diluted and concentrated Pr:KLM. Excitation wavelength: 450 nm. The observed transition is schematized in the inset of the figure.

$$^3P_0,\ ^3H_4 \rightarrow {}^1G_4,\ ^1G_4,$$

$$^1D_2,\ ^3H_4 \rightarrow {}^1G_4,\ ^3F_4,$$

illustrated in Fig. 4. In the $^3P_0$ case (Fig. 4(a)) the process is not resonant, since the two involved transitions occur at energies differing by about 950 cm^{-1}. It is then expected to be favoured by phonon assistance, since phonons of suitable energy are available in the Raman spectrum. Moreover, this mechanism is concomitant with the $^3P_0 \rightarrow {}^1D_2$ multiphonon relaxation. It can then be concluded that the emission from $^3P_0$ should be significantly temperature dependent. At variance, the cross-relaxation involving the $^1D_2$ state (Fig. 4(b)) is a nearly resonant process; then we have to expect a strong concentration and a weak temperature dependence. Another possible process that can contribute to the non-radiative depopulation of the $^3P_0$ and/or $^1D_2$ level involves the electron transfer

$$\mathrm{Pr}^{3+} + \mathrm{Mo}^{6+} \rightarrow \mathrm{Pr}^{4+} + \mathrm{Mo}^{5+},$$

and therefore an IVCT state that can provide, depending on its position, an efficient de-excitation channel for one or both emitting states. Experimental evidences of the presence of an IVCT state can be found in the excitation spectra, where it gives rise to a band located at lower energy with respect to the CT band of the host [6], and in a characteristic temperature behaviour of the integrated intensities of the emission bands, indicating a thermally induced crossover to a quenching state [5]. In the present case, the excitation spectrum of the Pr^{3+} emission in the 250–400 nm region (not shown here for brevity) is nearly identical to that of Fig. 1 and no extra bands are present that can be ascribed to IVCT transitions.

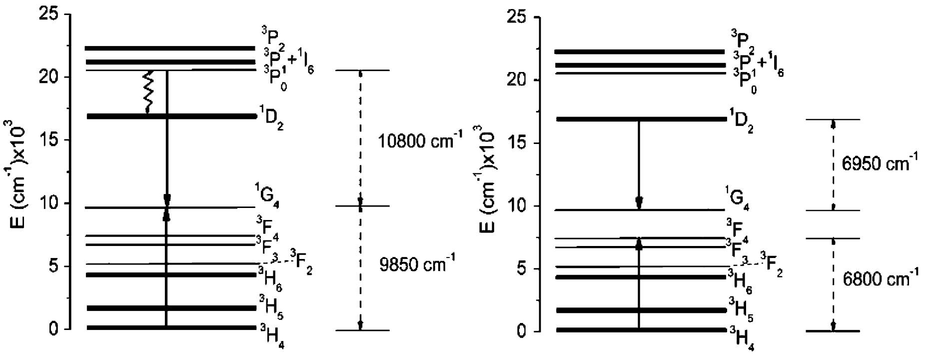

Fig. 4. Cross-relaxation schemes for the $^3P_0$ and $^1D_2$ levels.

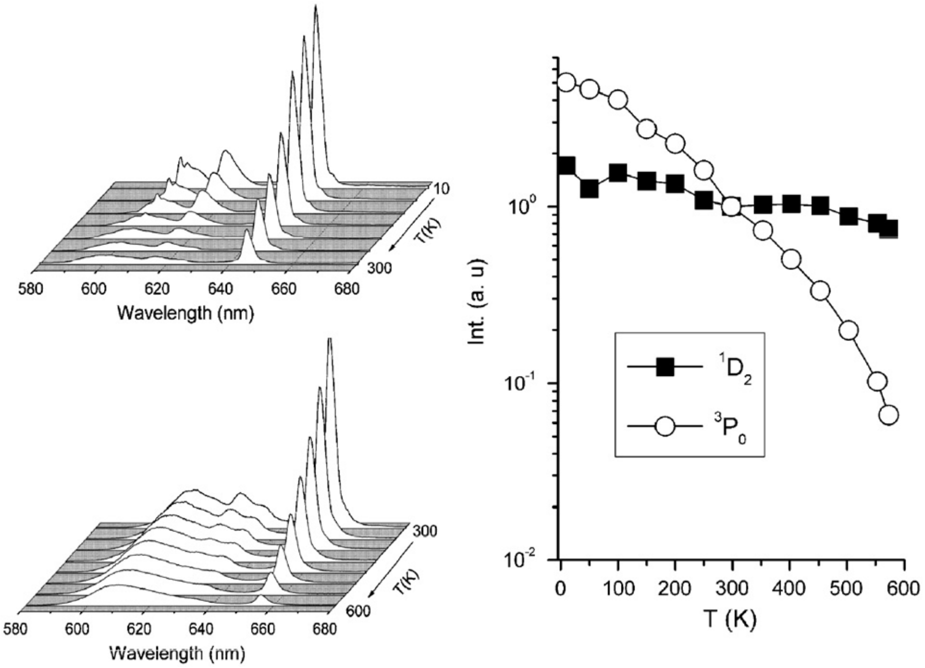

Fig. 5. Temperature behaviour of the Pr:KLM red emission upon 450 nm excitation.

3.3. Temperature behaviour of the luminescence

The 580–680 nm emission spectra of diluted Pr:KLM have been monitored as a function of the temperature in the 10–600 K range, divided for practical reasons into the 10–300 and 300–600 K sub-ranges. The integrated intensities of the observed features have been normalised with respect to the 300 K emission. The results obtained with excitation at 450 nm (in the $^3P_2$ state) are shown in Fig. 5. The intensity of the $^1D_2$ emission is nearly constant in the 10–600 K range, whereas that of the $^3P_0$ emission significantly decreases in agreement with the expected behaviour for the cross-relaxation processes. The $^3P_0$ temperature profile cannot be reproduced using the model proposed by Struck and Fonger for the case of crossover to a Franck–Condon shifted state [11], suggesting that no crossover to IVCT quenching states occurs for this level. We have also measured the spectra upon 320 nm excitation (Fig. 6). At low temperature the Pr^{3+} emission lines overlap the broadband host luminescence. The dips located in correspondence of the absorption transitions indicate that the energy transfer process is at least in part radiative. The relative intensities of the 610 and 650 nm emission features are different from the 450 nm excited spectra, since in this case they depend also on the relative values of the overlap integrals between the host emission and the absorption transitions to the $^3P_0$ and $^1D_2$ states. The temperature behaviour of the integrated intensities of the Pr^{3+} features generally agrees with that described above. We have also measured the decay profiles of the $^1D_2$ emission as a function of the temperature. They are not exponential and cannot be reliably fitted using a model based on a single energy transfer mechanism. This is probably an effect of the presence of many slightly different optical centres. We have then determined the average decay times using the following formula [12]:

$$\tau_{\text{avg}} = \frac{\int tI(t)\,\mathrm{d}t}{\int I(t)\,\mathrm{d}t}. \qquad (1)$$

They range from 30 μs at 10 K to about 55 μs at 298 K, confirming again the limited effect of the temperature on the $^1D_2$ emission efficiency. Unfortunately, it has not been possible to measure the temporal profiles of the $^3P_0$ emission since its decay time is very short, i.e. below the limit of our detecting system.

4. Discussion

No effects ascribable to the formation of an IVCT state have been observed, similarly to the case of Tb^{3+}-doped KLM. This is quite unexpected in the light of the results reported by Reut and Ryskin [4] concerning a number of scheelite-type oxides activated with Pr^{3+}. In this connection, we have to consider that the electron transfer giving rise to the IVCT state depends on the structural properties of the host and on the electronic properties of the involved ions, and that such dependence has not yet been formalised in a reliable theoretical model. In order to account for the observed behaviour, we have applied the phenomenological model proposed in Ref. [13], according to which the observed position of the IVCT band linearly depends on the ratio between the optical electronegativity ($\chi_{\text{opt}}(M^{n+})$) of the d^0 transition metal ion and its shortest distance ($d_{\text{min}}(Pr^{3+}–M^{n+})$) from the lanthanide ion. The data

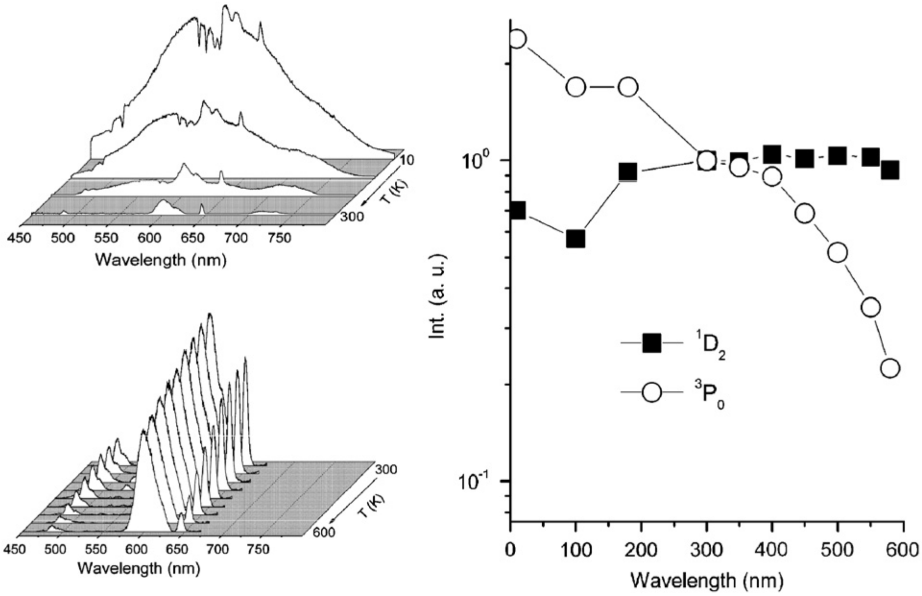

Fig. 6. Temperature behaviour of the Pr:KLM red emission upon 320 nm excitation.

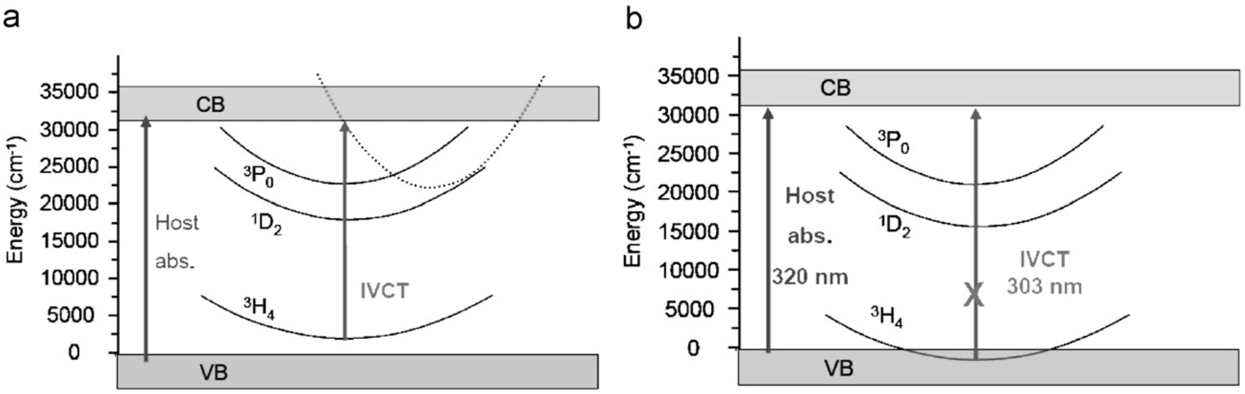

Fig. 7. (a) The general model for the IVCT mechanism and (b) the Pr:KLM case.

presented in Fig. 4. of Ref. [13] can be reproduced by the following equation:

$$\mathrm{IVCT}(\mathrm{Pr}^{3+}, \mathrm{cm}^{-1}) = 58\,800 - 49\,800\left(\frac{\chi_{\mathrm{opt}}(M^{n+})}{d_{\min}(\mathrm{Pr}^{3+} - M^{n+})}\right), \tag{2}$$

which allows to evaluate the expected energy position of the IVCT transition. In Pr:KLM its value is 33 000 cm^{-1} (303 nm). Even if relatively high, it is not very different from that found for several hosts, like niobates, in which there is partial quenching of the $^3P_0$ blue emission through crossover to an IVCT state. The absence of the IVCT transition in our case can be qualitatively accounted for by considering the model recently proposed by Krumpel et al. [14], who describes the IVCT process as an excitation from the ground state of Pr^{3+} to the conduction band of the host with the subsequent creation of a bound exciton connected to the formation of the Pr^{4+}–Mo^{5+} pair (Fig. 7(a)). In agreement with the excitation spectra, this transition occurs when the Pr^{3+} ground state is above the top of the valence band. In the case of KLM the host absorption occurs at lower energy than the predicted IVCT absorption, the ground state of the active ion is located below the top of the valence band of the host and the IVCT process cannot be observed (Fig. 7(b)). We can qualitatively connect this model to the phenomenological Eq. (2) by considering that the optical electronegativity is related to the bandgap of the compound, which is controlled by the transition metal cation, whereas the shortest Pr^{3+}–Mo^{6+} relates to the size of the site occupied by Pr^{3+}, and then to the position of its energy levels inside the bandgap. In the case of Tb:KLM [6] no IVCT is present, and moreover, the $^5D_3$ emission is observed at 10 K but it disappears above 250 K. This indicates that this level must be located just below the molybdate band. Therefore, the Tb^{3+} ground state is at most few tenths of eV above the valence band and consequently the IVCT transition cannot be discriminated from the host absorption. From these considerations it is possible to locate the energy levels of

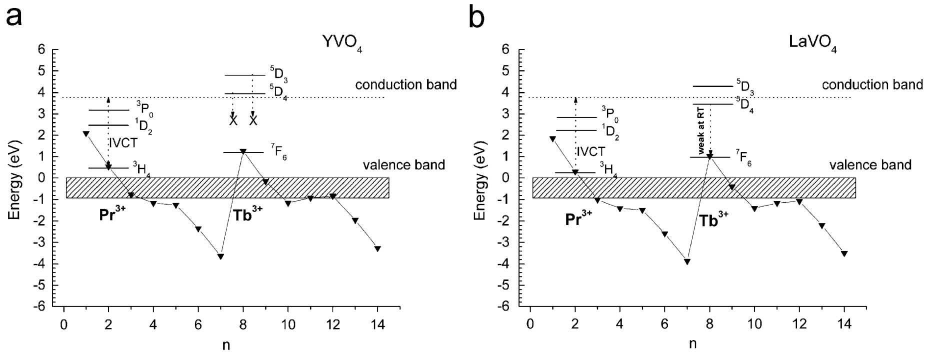

Fig. 8. Position of the ground state energy along the Ln^{3+} series in YVO_4 (a) and $LaVO_4$ (b).

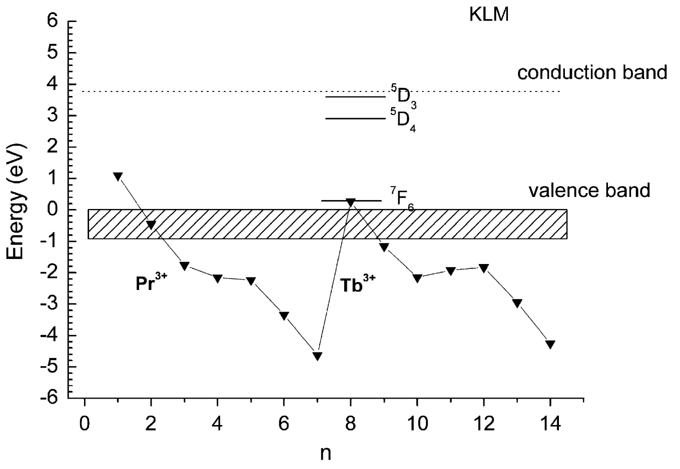

Fig. 9. Position of the ground state energy along the Ln^{3+} series in KLM.

Pr^{3+}, Tb^{3+} and then of the other trivalent lanthanide ions with respect to the valence and conduction bands of KLM using the procedure described in the following for the representative cases of YVO_4 and $LaVO_4$ doped with Pr^{3+} or Tb^{3+}, whose spectroscopic properties have been thoroughly investigated [14–16] and the IVCT effects well assessed. In Tb^{3+}:YVO_4 the vanadate absorption band is located at an energy that is similar to the one of MoO_4^{2-} in KLM. There is no $^5D_3$ nor $^5D_4$ emission from Tb^{3+}, even at low temperature, since the $^5D_4$ state is located above the vanadate band leading to spontaneous ionisation and total quenching of the emission. From the location of the Tb^{3+} levels those for Pr^{3+} and for the other trivalent rare earth can be reliably estimated by applying the empirical ‘double seat’ model proposed by Dorenbos [17]; the results limited to the ground state energies (with the exception of Pr^{3+} and Tb^{3+}) are shown in Fig. 8(a). The thus found location of the Pr^{3+} ground state is consistent with the observed energy of the IVCT band of Pr^{3+} in YVO_4 [15]. At 298 K, Tb^{3+}:$LaVO_4$ does not emit from $^5D_3$ and only weakly from $^5D_4$. This indicates that the $^5D_3$ level is above and the $^5D_4$ one just below the vanadate band, whose energy is similar to that in YVO_4. The Tb^{3+} levels in $LaVO_4$ are then at lower energy than in YVO_4 (see Fig. 8(b)). This is most likely related to the larger site of La^{3+} leading to a smaller Madelung potential at that site as compared to YVO_4. Again, once the location of the Tb^{3+} levels is known it is possible to deduce the one of the levels of Pr^{3+}, that is in agreement with the observed energy of the IVCT state [14], and of the other rare earth ions. This procedure can be easily applied to the case of KLM, giving rise to the energy level scheme reported in Fig. 9.

5. Conclusions

KLM crystals activated with Pr^{3+} have been grown and their emission spectra have been measured as a function of the temperature and of the excitation wavelength for two different doping levels. The effect of the host properties on the emission features has been evidenced. The temperature dependence of the emitted intensities has been accounted for on the basis of multiphonon relaxation and energy transfer mechanisms, allowing to exclude crossover to IVCT states. The excited state dynamics of the title compound has then been examined in the light of previous results concerning Tb:KLM and other Tb^{3+}- or Pr^{3+}-doped materials. It has been evidenced that the spectroscopic behaviour, in particular the presence or absence of IVCT processes, is related to the position of the energy levels of the optically active ions with respect to the bandgap of the host. Using the Dorenbos ‘double seat’ empirical model it has been possible to locate also the levels of the other rare earth ions. We think that this is a quite interesting aspect, since there is a number of open questions deserved to be discussed in the light of this information, regarding, for instance, the relative efficiencies of different lattices activated with the same luminescent ion, and so on. This is our challenge for the future, together with the development of a model, which allows relating the structural properties of the host with the presence and position of the IVCT states.

References

[1] E. Cavalli, E. Zannoni, C. Mucchino, V. Carozzo, A. Toncelli, M. Tonelli, M. Bettinelli, J. Opt. Soc. Am. B 16 (1999) 1958.
[2] E. Cavalli, C. Meschini, A. Toncelli, M. Tonelli, M. Bettinelli, J. Phys. Chem. Solids 58 (1997) 587.
[3] Y. Ye, X. Long, W. Lin, J. Li, G. Wang, Opt. Mater. (2007).
[4] E.G. Reut, A.I. Ryskin, Phys. Status Solidi (a) 17 (1973) 47.

[5] P. Boutinaud, P. Putaj, R. Mahiou, E. Cavalli, A. Speghini, M. Bettinelli, Spectros. Lett. 40 (2007) 209.
[6] P. Boutinaud, R. Mahiou, E. Cavalli, M. Bettinelli, Chem. Phys. Lett. 418 (2006) 185.
[7] E. Cavalli, P. Boutinaud, T. Cucchietti, M. Bettinelli, Opt. Mater., doi:10.1016/j.optmat.2007.10.021.
[8] G. Blasse, Structure and bonding 42 (1980).
[9] K. Nakamoto, Infrared and Raman Spectra of Inorganic Compounds, Wiley, New York, USA, 1997.
[10] L. Macalik, J. Hanuza, J. Sokolnicki, J. Legendziewicz, Spectrochim. Acta A 55 (1999) 251.
[11] C.W. Struck, W.H. Fonger, J. Appl. Phys. 42 (1971) 4515.
[12] W.M. Yen, Phosphor Handbook, CRC Press, Boca Raton, USA, 2000.
[13] P. Boutinaud, R. Mahiou, E. Cavalli, M. Bettinelli, J. Lumin. 122–123 (2007) 430.
[14] A. Krumpel, E. van der Kolk, P. Dorenbos, P. Boutinaud, E. Cavalli, M. Bettinelli, Mater. Sci. Eng. B 146 (2008) 114.
[15] P. Boutinaud, R. Mahiou, E. Cavalli, M. Bettinelli, J. Appl. Phys. 96 (2004) 4923.
[16] R.G. DeLosh, T.Y. Tien, E.F. Gibbons, P.J. Zacmanidis, H.L. Stadler, J. Chem. Phys. 53 (1970) 681.
[17] P. Dorenbos, J. Phys. Condens. Matter 15 (2003) 8417.